doi:10.1016/j.jmb.2009.11.076 J. Mol. Biol. (2010) 396, 646–662

JMB

Available online at www.sciencedirect.com

ScienceDirect

ELSEVIER

The cAMP Receptor-Like Protein CLP Is a Novel c-di-GMP Receptor Linking Cell–Cell Signaling to Virulence Gene Expression in *Xanthomonas campestris*

Ko-Hsin Chin[1,2], Yen-Chung Lee[1], Zhi-Le Tu[1], Chih-Hua Chen[3], Yi-Hsiung Tseng[4], Jinn-Moon Yang[5], Robert P. Ryan[6], Yvonne McCarthy[6], J. Maxwell Dow[6], Andrew H.-J. Wang[7] and Shan-Ho Chou[1,2]*

[1]*Institute of Biochemistry, National Chung-Hsing University, Taichung 40227, Taiwan, ROC*

[2]*National Chung Hsing University Biotechnology Center, National Chung-Hsing University, Taichung 40227, Taiwan, ROC*

[3]*Institute of Molecular Biology, National Chung-Hsing University, Taichung 40227, Taiwan, ROC*

[4]*Institute of Microbiology, Immunology, and Molecular Medicine, Tzu Chi University, Hualien 970, Taiwan, ROC*

[5]*Institute of Bioinformatics and Systems Biology, National Chiao-Tung University, Hsin-Chu 30010, Taiwan, ROC*

[6]*BIOMERIT Research Center, Department of Microbiology, BioSciences Institute, University College Cork, Cork, Ireland*

[7]*Institute of Biological Chemistry, Academia Sinica, Nankang 115, Taipei, Taiwan, ROC*

Received 6 October 2009; received in revised form 23 November 2009; accepted 24 November 2009
Available online 18 December 2009

Edited by R. Huber

Cyclic-di-GMP [bis-(3′-5′)-cyclic diguanosine monophosphate] controls a wide range of functions in eubacteria, yet little is known about the underlying regulatory mechanisms. In the plant pathogen *Xanthomonas campestris*, expression of a subset of virulence genes is regulated by c-di-GMP and also by the CAP (catabolite activation protein)-like protein *Xc*CLP, a global regulator in the CRP/FNR superfamily. Here, we report structural and functional insights into the interplay between *Xc*CLP and c-di-GMP in regulation of gene expression. *Xc*CLP bound target promoter DNA with submicromolar affinity in the absence of any ligand. This DNA-binding capability was abrogated by c-di-GMP, which bound to *Xc*CLP with micromolar affinity. The crystal structure of *Xc*CLP showed that the protein adopted an intrinsically active conformation for DNA binding. Alteration of residues of *Xc*CLP implicated in c-di-GMP binding through modeling studies caused a substantial reduction in binding affinity for the nucleotide and rendered DNA binding by these variant proteins insensitive to inhibition by c-di-GMP. Together, these findings reveal the structural mechanism behind a novel class of c-di-GMP effector proteins in the CRP/FNR superfamily and indicate that *Xc*CLP regulates bacterial virulence gene expression in a manner negatively controlled by the c-di-GMP concentrations.

Keywords: *Xcc*; pathogenicity; CRP; CLP; c-di-GMP receptor

**Corresponding author.* Institute of Biochemistry, National Chung-Hsing University, Taichung 40227, Taiwan, ROC. E-mail address: shchou@nchu.edu.tw.

Abbreviations used: c-di-GMP, [bis-(3′-5′)-cyclic diguanosine monophosphate]; *Xcc*, *Xanthomonas campestris* pv. *Campestris*; DSF, diffusible signal factor; CAP, catabolite activation protein; EMSA, electrophoretic mobility shift assay; SPR, surface plasmon resonance; ITC, isothermal titration calorimetry; HTH, helix–turn–helix.

Introduction

Cyclic-di-GMP [bis-(3′-5′)-cyclic diguanosine monophosphate] is an important novel secondary messenger involved in modulating a variety of biological activities in eubacteria.[1–4] In the plant pathogen *Xanthomonas campestris* pv. *campestris* (*Xcc*), c-di-GMP is implicated as a second messenger controlling expression of pathogenicity genes in response to the extracellular diffusible signal factor DSF.[5–8] DSF signal transduction involves the hybrid sensor kinase RpfC and the response regulator RpfG. DSF perception by RpfC is believed to lead to its autophosphorylation and subsequent phosphorelay to RpfG. RpfG is unique in that it contains no DNA-binding domain, but an HD-GYP domain that exhibits phosphodiesterase activity capable of degrading c-di-GMP to GMP.[6,7,9–13] Phosphorylation is thought to activate RpfG for c-di-GMP degradation. In this way, RpfC/RpfG link perception of the cell–cell signal DSF to alteration in the cellular level of c-di-GMP. What is not clear, however, is how alteration in c-di-GMP levels is coupled to the downstream pathogenicity gene expression that is under DSF control.

Recently, a number of studies have strongly suggested that *Xc*CLP, a global transcriptional regulator with an N-terminal β-barrel domain and a C-terminal DNA-binding domain, plays a key role in the DSF-mediated regulatory pathways in *Xcc*.[9,14,15] Although *Xc*CLP was originally named due to its high sequence similarity with the well-known catabolite activation protein (CAP, also known as CRP due to its function as a cAMP receptor protein),[16–19] it does exhibit functions that differ considerably from those of *Ec*CRP; knockout of this protein in *Xcc* does not affect the utilization of some carbon sources, but significantly alters the expression profile of a number of pathogenicity factors such as exopolysaccharide, extracellular cellulase, and polygalacturonate lyase.[16,20–23] These data together with more recent transcriptome profiling analysis reveal that *Xc*CLP regulates expression of a subset of genes of the Rpf/DSF regulon. The mechanistic link between *Xc*RpfG and *Xc*CLP in pathogenicity gene regulation has, however, remained obscure.[9,14,24]

In this article, we report the crystal structure of *Xc*CLP determined by X-ray crystallography and show that it belongs to the CRP/FNR superfamily.[25,26] We also show that *Xc*CLP is unique in this superfamily because it is intrinsically adapted for DNA binding without the need for any ligand. Furthermore, *Xc*CLP is found to be released from DNA binding when incubated with c-di-GMP in competition electrophoretic mobility shift assay (EMSA) and surface plasmon resonance (SPR) assay, indicating that c-di-GMP acts as a negative regulator for downstream pathogenic gene expression via changing *Xc*CLP conformation. *Xc*CLP was also shown to directly bind c-di-GMP with a K_D of approximately 3.5 μM by an isothermal titration calorimetry (ITC) experiment. *Xc*CLP is thus likely to be one of the long sought-after c-di-GMP receptor proteins in the DSF-mediated pathways.[2,15] It may serve as a checkpoint for controlling expression of virulence factors in response to extracellular signals such as DSF or intracellular conditions that act to modulate the cellular level of c-di-GMP.

Results

Preparation and characterization of native and variant *Xc*CLPs

Figure 1a shows the sequence and structural alignment between *Xc*CLP and *Ec*CRP. Although these two proteins bear considerable sequence identity (~44%), some crucial residues have been altered. These residues are highlighted in pink, blue, and orange, and the significant conformational changes triggered by these residues are described in detail in the following sections. When expressed in *Escherichia coli*, *Xc*CLP was found to be difficult to dissolve. A higher salt concentration of 250 mM NaCl and 100 mM LiCl in 20 mM Tris (pH 8.0) buffer is necessary to increase the solubility up to 10 mg/ml. The active form of *Xc*CLP was confirmed by using an EMSA experiment (Fig. 1b). Previously, we have shown that the *engA* promoter upstream region contains two *Xc*CLP-binding sites (designated sites I and II).[22] We thus used this DNA fragment as a probe for the EMSA analysis. As shown in Fig. 1b, an apparent DNA–protein complex was detected for *Xc*CLP (lane 2), which migrated at a slower rate than the control probe (lane 1). Furthermore, the amount of complexes increases from 4 to 8 μM per reaction (lane 2 *versus* lane 3) of *Xc*CLP. The binding affinity of *Xc*CLP for the *engA* promoter DNA was also quantitated by an SPR method as shown in Fig. 1c. A dissociation constant (K_D) of approximately 14 nM at low salt buffer or 0.36 μM at high salt buffer (Table 1) was obtained when these curves were fitted using the BIAevaluation software supplied by the vendor. The value obtained at low salt buffer is close to the K_D value estimated from a wild-type *Xc*CLP concentration-dependent EMSA experiment carried out before in our laboratory.[22] In addition to native *Xc*CLP, we also prepared a series of variants with single, double, and triple alanine substitutions to confirm the roles played by specific residues in DNA and c-di-GMP binding using ITC and SPR assays.

Global structure of *Xc*CLP

Using the new solubility condition described above, we were finally able to grow the *Xc*CLP crystals that diffracted to a resolution of 2.28 Å. They were found to belong to the monoclinic space group P_{21}, with unit cell parameters of $a = 67.687$ Å, $b = 67.694$ Å, and $c = 110.372$ Å, $\beta = 104.20°$. Two dimers with a molecular mass of approximately 52 kDa are present per asymmetric unit with a

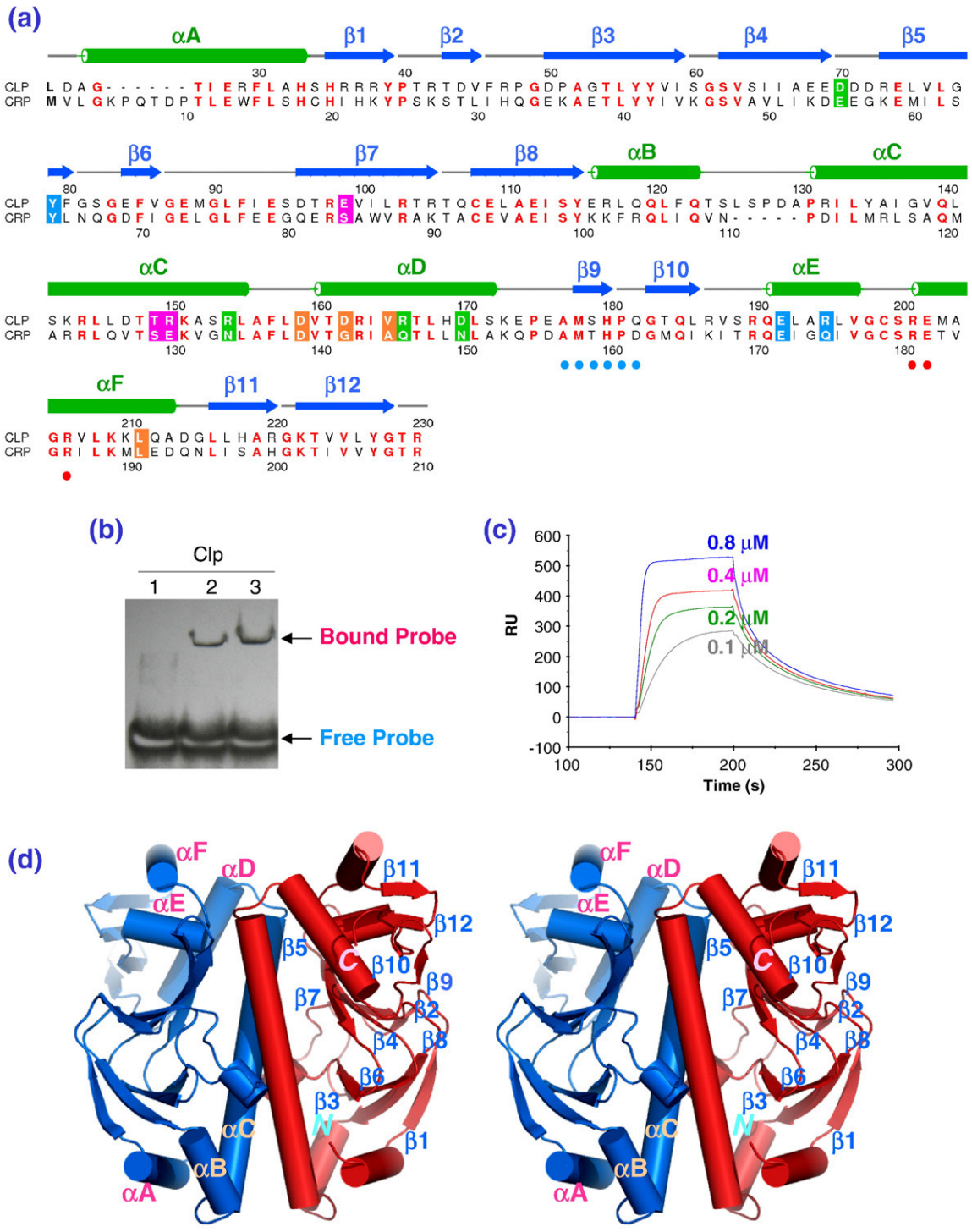

Fig. 1. Characterization of the *Xc*CLP protein. (a) A structure-based sequence alignment of *Xc*CLP and *Ec*CRP. The secondary structural elements of *Xc*CLP are schematically shown above the alignment, with α-helices rendered as green cylinders and β-strands as blue arrows. Identical residues are shown in red. Residues participating in unique H-bonds or salt bridges for stabilizing the intrinsically active DNA-binding conformation for sites A, B, and C of *Xc*CLP are highlighted in red, blue, and orange, respectively. Residues forming salt bridges with c-di-GMP from a model study are highlighted in green. Residues located in helix αF and participating in DNA-binding in *Ec*CRP are marked with red dots, while those participating in binding the C-terminal peptide of RNA polymerase are marked with blue dots. (b) Binding of *Xc*CLP to *engA* promoter at two different CLP concentrations of 4 μM (lane 2) and 8 μM (lane 3), respectively. (c) Binding curves of SPR experiment at different concentrations of *Xc*CLP using a biotin-labeled *engA* promoter DNA-coated chip. (d) The global structure of *Xc*CLP dimer. One subunit was colored red, while another was colored blue. The secondary structures of α-helices are rendered as cylinders and sequentially marked by letters (left-hand subunit), while β-strands are rendered as curved arrows and sequentially marked by numbers (right-hand subunit). The N- and C-termini of the right subunit are also labeled with green N and C letters, respectively.

Table 1. Binding affinities of native and mutant CLPs with promoter DNA determined by SPR under low salt and high salt buffer conditions

	Low salt[a]		High salt[b]	
	K_D (M)[c]	Fold	K_D (M)[c]	Fold[d]
Native CLP	1.40E-08	1.0	3.62E-07	25.8
K173A/E174A/E176A	1.56E-08	1.1	4.19E-7	26.9
E99A	4.45E-07	31.8	ND	
R150A	1.96E-07	14.0	ND	
E99A/R150A	5.72E-06	408.6	ND	
R195A	3.60E-07	25.8	ND	
D162A	1.75E-07	12.5	ND	
V165A	2.35E-07	16.8	ND	
D70A	2.80E-08	2.0	ND	
R154A	1.90E-08	1.4	ND	
R166A	2.56E-08	1.8	ND	
D170A	1.70E-08	1.2	ND	
R166A/D170A	2.52E-08	1.8	ND	

ND, non-determined.
[a] Low-salt buffer: 80 mM NaCl, 20 mM Tris (pH 8.0), and 20 mM LiCl.
[b] High-salt buffer: 250 mM NaCl, 20 mM Tris (pH 8.0), and 100 mM LiCl.
[c] Average values from three separate runs.
[d] The ratio between high salt and low salt K_D values.

solvent content of 49.25%. Since sequence identity between the *Xc*CLP and *Ec*CRP proteins is rather high (~44%), we used the *Ec*CRP structure in the *Ec*RCP–DNA–cAMP complex [Protein Data Bank (PDB) code 2CGP] as the template to determine the protein phases by a molecular replacement methodology.[27,28] The final result indicates that the apo *Xc*CLP structure is roughly similar to the *Ec*CRP structure in the *Ec*CRP–cAMP–DNA complex,[18] even when *Xc*CLP was crystallized in the absence of either cAMP or DNA. The electron density map was rather clear (see Supplementary Fig. S1) and the model could be well fit throughout the sequence except for the first 21 N-terminal residues, the last Arg residue, and a few loop residues, such as K173, E174, and E176, the side chains of which remain invisible even after repeated iterative refinement, possibly due to the higher flexibility in this region. *Xc*CLP is found to adopt a dimeric structure similar to the other members in the CRP/FNR superfamily,[26] comprising an N-terminal domain (residues 21–127) and a C-terminal DNA-binding domain (residues 158–230) linked by a dimerization domain consisting of a long α-helix (residues 128–157) (Fig. 1d). The N-terminal domain is a classical eight-stranded antiparallel β-barrel (β1–β8) flanked by two α-helices (αA and αB). The C-terminal domain consists of three α-helices (αD–αF) and four antiparallel β-strands (β9–β12), with the two α-helices, αE (residues 191–197) and αF (201–213), and the connecting loop, αE–αF (198–200), constituting the well-known helix–turn–helix (HTH) motif as also observed in many other DNA-binding proteins (Fig. 1d). However, some notable differences between the *Xc*CLP and *Ec*CRP structures are evident. The most prominent one is that *Xc*CLP forms a mainly symmetrical dimer, with each subunit adopting a closed form suitable for DNA binding (Fig. 1d); no molecule other than *Xc*CLP and water was detected in the electron map. This is in marked contrast to *Ec*CRP,[19,29] which adopts a dimer of nonsymmetrical nature, with one subunit adopting an open form and another a closed form, even when it was crystallized in the presence of cAMP. It only formed a symmetrical dimer when crystallized in the presence of both cAMP and cognate DNA.[18]

The structural difference between the *Xc*CLP and the *Ec*CRP–cAMP complex is most obvious in the C-terminal DNA-binding domain, which was depicted in the superimposition figure of Fig. 2a. As clearly shown in the figure, when superimposition was carried out based on the A subunits, the conformations of the DNA-binding domains of the B subunits experience a considerable shifting; the DNA contacting helix αF of *Xc*CLP (colored red) was shifted rightward, with the whole C-terminal domain shifted downward toward the N-terminal domain compared to those of *Ec*CRP (indicated by cyan arrows in Fig. 2a). These movements decrease the gap between the N- and C-terminal domains, which is characteristic of a closed and active form of the *Ec*CRP–cAMP complex. It is intriguing to observe that the apo form of *Xc*CLP can assume an intrinsically active DNA-bound conformation without the need for conformational changes induced by an effector ligand bound to the N-terminal domain, which is the case for all other CRP/FNR superfamily proteins described so far.[26] Previous structural and functional studies have clearly shown that the DNA-binding activity of *Ec*CRP is greatly facilitated by conformational change associated with cAMP binding within the nucleotide-binding pocket located in the N-terminal β-barrel domain. The conformational change is then transmitted through the helical dimerization domain, the hinge region, and finally to the C-terminal HTH motif (colored by dotted orange lines and a curved yellow arrow in Fig. 2b).[30] How does apo *Xc*CLP form a similar active structure in the absence of cAMP induction? Through detailed

Fig. 2. *Xc*CLP adopts an intrinsically active DNA-binding comformation. (a) Superimposition between the DNA-binding domains of *Xc*CLP (red) and *Ec*CRP–cAMP (blue) in ribbon representation. The significant shifting of helices αD, αF, and β-strands β9–β12 is obvious from this figure (indicated by green arrows). Cartoon representations of (b) the global structure of *Ec*CRP and (c) the corresponding *Xc*CLP structure. (d) Line drawing of the superimposition of global structures of *Xc*CLP and *Ec*CRP–cAMP. The left subunits A of both structures are shown in gray, while the right subunit B of *Xc*CLP is shown in red and that of *Ec*CRP in blue. The cAMPs in *Ec*CRP are shown in stick representation. The three interaction sites (sites A, B, and C) important for maintaining an active DNA-bound conformation for *Xc*CLP are circled in red, blue, and orange and are enlarged as close-ups in Fig. 3a–c, respectively. The modeled region putatively important for c-di-GMP binding was circled in green (site D) and expanded in Fig. 5.

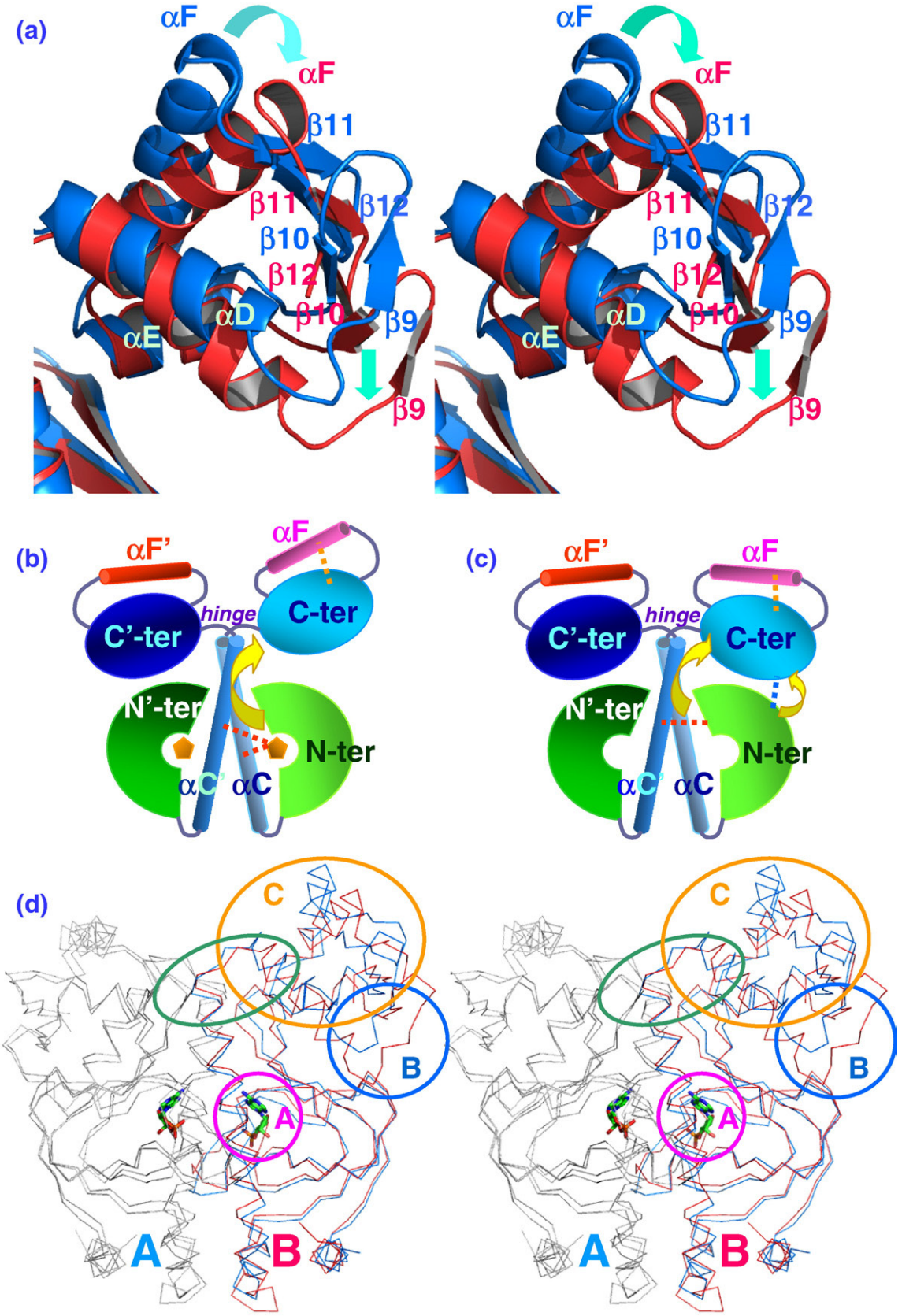

Fig. 2 (*legend on previous page*)

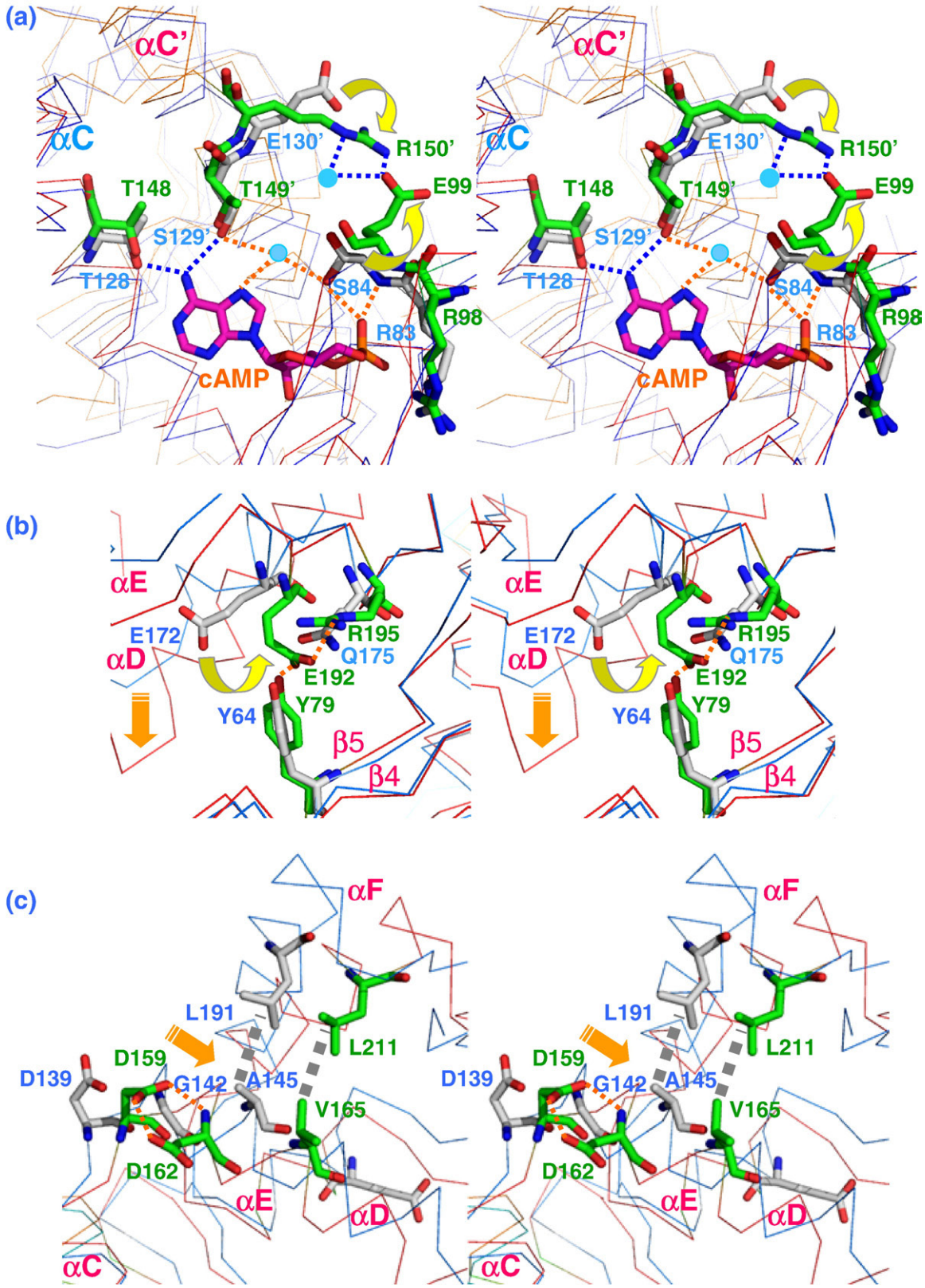

Fig. 3. Close-up of important interaction sites of *Xc*CLP compared to those in *Ec*CRP–cAMP. (a) Site A, (b) site B, and (c) site C. Residues participating in specific interactions are drawn in stick representation, with nitrogen atoms colored blue, oxygen atoms red, and carbon atoms green for *Xc*CLP and gray for *Ec*CRP. The carbon atoms of cAMP for *Ec*CRP are colored pink. Residues are labeled in blue letters for *Ec*CRP and in green letters for *Xc*CLP. Residues from opposing subunits are further labeled with a prime. H-bonds or salt bridges are marked with dotted lines, while hydrophobic interactions in (c) are marked with thicker dotted gray lines. Side chains experiencing crucial rotations are indicated by curved yellow arrows, and domain shifting is indicated by orange arrows.

structural studies, we have identified three unique locations (sites A, B, and C) in apo *Xc*CLP that appear to be crucial in carrying out this structural communication pathway. These regions are shown as red, blue, and orange circles in Fig. 2d, and interactions between these regions are shown in cartoon representation in Fig. 2c and annotated by a dotted red line, a dotted blue line, and a dotted orange line, respectively. The extensive molecular interactions in these locations are further shown expanded in Fig. 3a–c for closer examination. While site A represents the region experiencing conformational changes due to alteration of residues affecting interaction between the N-terminal cyclic nucleotide binding domain and the dimerization helical (αC) domains, site B represents those residue changes affecting interaction between the N-terminal and the C-terminal DNA-binding domains, and site C represents those residue changes affecting interaction between the dimerization domain and the DNA-binding domain. Altogether, we believe that these structural changes culminate in rearrangement of the *Xc*CLP HTH motif, allowing it to adopt a proper conformation suitable for target DNA binding.

Close-up of site A region

Figure 3a shows the stereo superimposition of the effector binding motifs in the *Xc*CLP and *Ec*CRP–cAMP structures. In this region, most of the residues are similar and their backbones well superimposed, except for the two crucial residues, S84 and E130′ (primed residues are from the neighboring subunit) in *Ec*CRP, corresponding to E99 and R150′ in *Xc*CLP, respectively. The results of these two mutations have, however, elicited dramatic change in the side chains of these two residues (indicated by curved yellow arrows in Fig. 3a, with the electron density of the *Xc*CLP site A depicted in Supplementary Fig. S1a) and associated changes in the capability of *Xc*CLP to bind cAMP. This is consistent with the previous report that cAMP exhibited no effect on the growth of *X. campestris* and binding of cAMP to *Xc*CLP was very weak (K_a ~15 mM).[16] Previous data have shown that S84 residue is the most crucial residue in positioning the cAMP ligand in *Ec*CRP.[19] It forms a direct H-bond with the O1P atom of cAMP and an indirect H-bond with the N7 atom of cAMP through a bridging water molecule, which also forms a H-bond with the side-chain atom of S129′ from helix αC′ of the dimerization domain. The O1P atom further forms a H-bond with the backbone N atom of R83. Thus, the single key residue S84 alone positions the cAMP effector in the *Ec*CRP–cAMP complex structure through five direct or indirect H-bonds (indicated by red dotted lines in Fig. 3a). However, in *Xc*CLP, the corresponding residue is a larger and negatively charged residue, E99. Also, the corresponding residue of the nearby negatively charged E130′ in *Ec*CRP is positively charged (R150′) in *Xc*CLP. The alternative interaction between the S84–S129′ pair in *Ec*CRP and the E99–E130′ pair in *Xc*CLP seems to dramatically change the local environment of the cAMP binding pocket, accounting for the abolishment of the cAMP-binding capability of *Xc*CLP. This effect is due to the flipping of the E99 side chain away from the ligand binding site (indicated by a curved yellow arrow in Fig. 3a) and the rotation of the side chain of R150′ toward E99, allowing these two nearby residues to form a new salt bridge. Besides, a water molecule was found to bridge the side chains of R150′ and E99 by forming two H-bonds with the R150′N^{ε} and the E99$O^{\varepsilon 1}$ atoms, respectively (see Fig. 3 and Supplementary Fig. S1). The mutation of S84 to E99 in the cyclic nucleotide binding pocket removes a key functional group and causes structural changes that lead to a loss of all five H-bonds present in the *Ec*CRP protein. This can account for the very weak binding of cAMP within this pocket. Since it is generally believed that cAMP binding to residue T128 in the helix αC and to residue S129′ in the helix αC′ is essential for transmitting the conformational changes emanating from the nucleotide-binding domain to the dimerization domain in *Ec*CRP,[19] the absence of effector binding in *Xc*CLP seems to be partially compensated for by the formation of the new E99–H_2O–R150′ salt bridge–H-bond network, which possibly achieves the similar transmission effect through residue R150′ located in helix αC′.

Close-up of site B region

Site B seems to control the dimension of the gap between the N-terminal and the C-terminal domains of *Xc*CLP within the same subunit. In this site, although only one corresponding residue is changed (Q175 to R195), this mutation nevertheless exerts considerable effect on reducing this gap dimension. As shown in Fig. 3b, alteration of this single residue from Q175 in *Ec*CRP to R195 in *Xc*CLP has caused the flipping of residue E192 in *Xc*CLP to form a salt bridge with the altered residue R195. The flipped residue E192 is found to further form a H-bond with residue Y79 located at the β5 strand in the N-terminal domain (the electron density of *Xc*CLP site B is depicted in Supplementary Fig. S1b). As a result, the gap dimension between the N-terminal and the C-terminal domains is now considerably reduced by approximately 6 Å to form a closed conformation (marked by a down orange arrow in Fig. 3b and circled blue in Fig. 2d).

Close-up of site C region

Site C is possibly the most crucial region in positioning the DNA-contacting HTH domain implicated in DNA binding. This also involves the hinge region that has been extensively investigated previously and found to confer *Ec*CRP* mutants the constitutive DNA-binding activity.[30,31] According to previous results, amino acid residues 139 (located within the hinge region) and 142 (located in the αD helix adjacent to the hinge) in *Ec*CRP* need to be polar to achieve the cAMP-independent transcrip-

tion by *Ec*CRP, suggesting the requirement for αC and αD helices to come together.[31] As a result, the αF helix is released from the αD helix to interact with DNA. Furthermore, it was found that residue 145 in the αD helix of *Ec*CRP* is crucial in interacting with the αF helix, and replacement of this residue by an amino acid with a bulky side chain, regardless of its nature, results in cAMP-independent DNA binding.[31] These two requirements are both fulfilled in the current *Xc*CLP sequence, as shown in Figs. 1a and 3c. The corresponding residue G142 of *Ec*CRP is indeed an asparate (D162) in *Xc*CLP, which forms two H-bonds with the side-chain atoms of residue D159 (marked by dotted red lines in Fig. 3c) to draw near the αC and αD helices. In addition, the corresponding residue A145 in the αD helix of *Ec*CRP is also changed to a rather bulky and hydrophobic residue (V165 in *Xc*CLP) to push and orient the αF helix for better DNA interaction (the electron density of *Xc*CLP site C is depicted in Supplementary Fig. S1c).

Thus, although *Xc*CLP shares a considerable sequence similarity with *Ec*CRP (~44%), and adopts a similar global structure, some subtle structural differences do exist due to the amino acid alterations at several crucial positions described above. These differences allow *Xc*CLP to adopt an intrinsically active DNA-bound conformation without the need of any ligand induction as has been described for related variants of *Ec*CRP*.[30] This contention is strongly supported by the good superimposition between the apo *Xc*CLP structure and the cAMP-induced *Ec*CRP structure in the *Ec*CRP–DNA complex (see Supplementary Fig. S2) and by the extensive SPR studies on variant *Xc*CLP proteins described below.

SPR studies confirm that E99, R150, R195, D162, and V165 residues are critical for *Xc*CLP binding to promoter DNA

As outlined above, the X-ray crystal structure of *Xc*CLP indicates that the residues E99, R150, R195, D162, and V165 are essential for the intrinsic capability of *Xc*CLP to bind promoter DNA. The role of these residues in DNA binding was examined directly by SPR experiments using variant *Xc*CLP proteins with alanine substitutions at these positions. As shown in Table 1 and Supplementary Fig. S3, *Xc*CLP variants E99A, R150A, R195A, D162A, and V165A bound promoter DNA less strongly than did the native protein, with K_D values ranging from 13- to 32-fold higher than for the native *Xc*CLP. The E99A/R150A double variant had a K_D that is approximately 400-fold higher than that of the native protein, indicating the potential cumulative influence of the identified residues for promoter DNA binding. In contrast, alanine substitutions of residues not predicted to be involved in DNA binding (including D70A, R154A, R166A, D170A, R166A/D170A double substitution, and the K173A/E174A/E176A triple substitution) had little or no effect on K_D values, which differ only by 1.2- to 2.0-fold from that of the native protein (Table 1). These SPR studies confirm the importance of the residues revealed from crystal structure for the intrinsic DNA-binding capability of *Xc*CLP.

c-di-GMP directly binds *Xc*CLP

Deletion of the *rpfG* gene in *Xcc* leads to elevated cellular levels of c-di-GMP[32] and coordinates down-regulation of expression of a number of pathogenicity genes, some of which are positively regulated by *Xc*CLP.[14,15] On the basis that *Xc*CLP adopts an intrinsically active conformation for DNA binding, we hypothesized that c-di-GMP binds *Xc*CLP and negatively influences the transcriptional capability of *Xc*CLP, thus linking c-di-GMP level with pathogenicity gene expression.

To test this scenario, we carried out a competition EMSA experiment, incubating the *Xc*CLP–DNA complex mixture with different amounts of c-di-GMP to see if c-di-GMP is able to affect *Xc*CLP binding to DNA. The results are shown in Fig. 4. First, three different DNA probes containing both site I and site II promoter sequences (probe a), containing only a single site II promoter sequence (probe b), and containing no promoter sequence (probe c), were designed.[22] The probe is used as a control because it contains no promoter sequence for efficient *Xc*CLP binding. This is shown in lane c of Fig. 4b, in which no *Xc*CLP–DNA complex is observed even when *Xc*CLP is present at an amount of 1000 ng. However, both probe a and probe b bind *Xc*CLP (the position of the *Xc*CLP–DNA complex is marked by gray arrows in Fig. 4b and c). The binding is stronger for probe a because it contains a tandem set of two promoter binding regions. *Xc*CLP can be dissociated from both *Xc*CLP–probe a and *Xc*CLP–probe b complexes when 10 μM c-di-GMP is present in the mixture. In Fig. 4c, different amounts of c-di-GMP are applied to the (more stable) *Xc*CLP–probe a complex to

Fig. 4. Interaction of *Xc*CLP with promoter DNA by competitive EMSA experiments of c-di-GMP against the *Xc*CLP–DNA complex and interaction of *Xc*CLP with c-di-GMP by ITC experiment. (a) PCR fragments used as probes in the current EMSA experiments. Positions of the probes are numbered relative to the translation initiation site of the *Xcc engA* gene. (b) Competitive EMSA experiments in the absence (indicated by a bar) or the presence of various amounts of CLP or c-di-GMP indicated above the figures using probes a, b, and c. Probe c was used as a control. (c) Competitive EMSA experiments using increasing amounts of c-di-GMP. (d) ITC: *Xc*CLP (25 μM) was titrated with c-di-GMP (0.375 mM) in binding buffer at 25°C. The power necessary to maintain a constant temperature during the titration experiment (microcalories per second), corresponding to the heat released upon binding, was measured over a series of 13 injections of c-di-GMP (left) and integrated over time to obtain a plot of enthalpy *versus* ligand–protein molar ratio (right).

assay the efficiency of c-di-GMP inhibition of DNA binding. It is clear that at 20 μM, c-di-GMP is able to almost completely inhibit *Xc*CLP from binding DNA probe a. This competitive EMSA experiment strongly suggests that c-di-GMP is able to bind *Xc*CLP to relieve it from binding cognate DNA

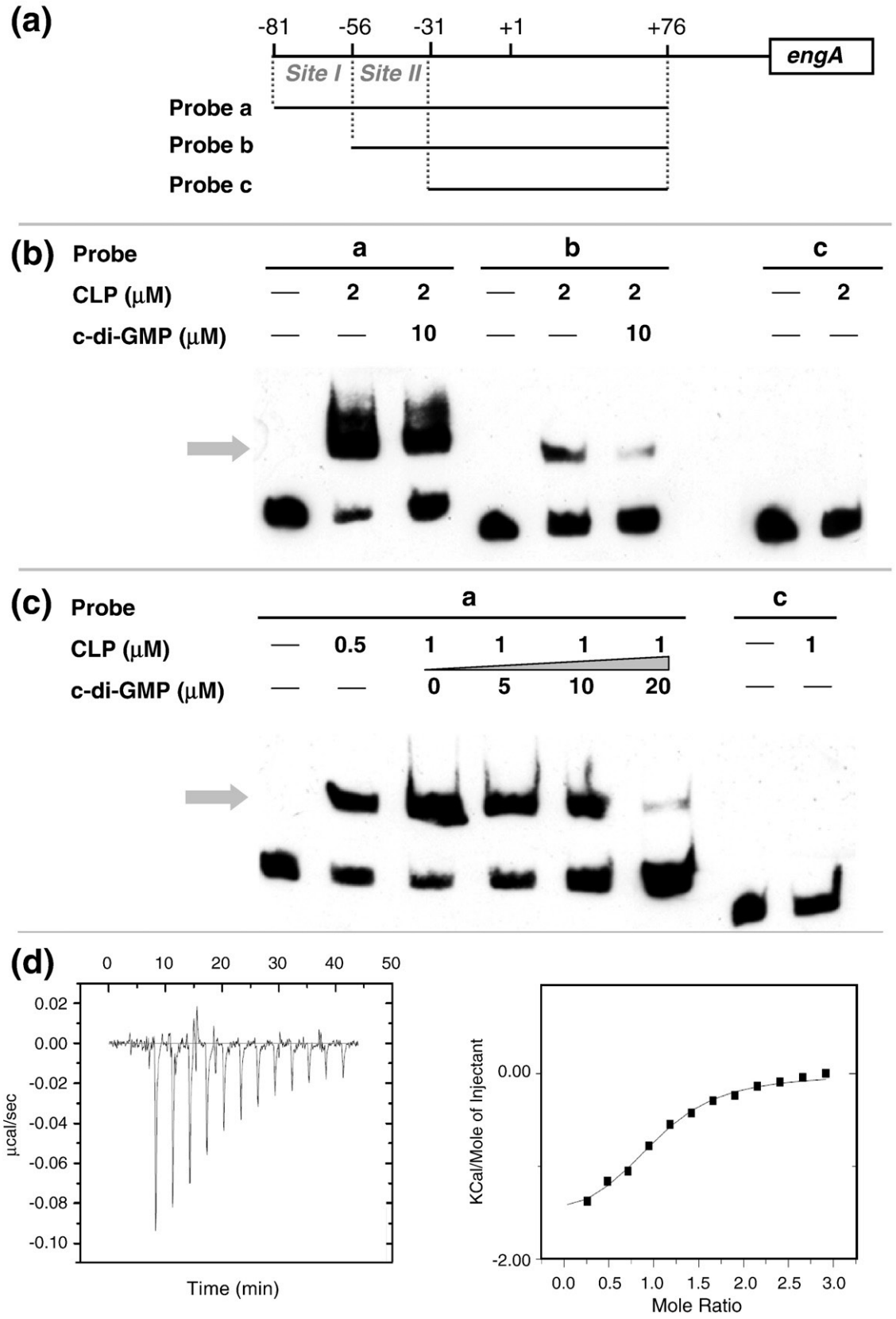

Fig. 4 (*legend on previous page*)

promoter and hence inactivate the downstream pathogenicity gene expression.

The inhibitory effect of c-di-GMP on *Xc*CLP binding to promoter DNA could be potentially exerted through binding of the nucleotide to promoter DNA, perhaps causing duplex distortion, or to *Xc*CLP. These possibilities were tested experimentally. SPR has been found to be sensitive enough to detect binding to double-stranded DNA for drugs with molecular mass as small as 300 Da.[33] Nevertheless, in SPR experiments in which solutions of c-di-GMP (690 Da) were passed over a promoter DNA chip, no binding of c-di-GMP to DNA was detected. On the contrary, *Xc*CLP was found to bind c-di-GMP in an ITC experiment. *Xc*CLP (200 μl of 25 μM solution at high salt buffer) was titrated with an injectant solution of 0.375 mM c-di-GMP at high salt buffer (3 μl each time) at 25°C and the heat released upon binding was measured by integration of power over a range of ligand concentrations (left, Fig. 4d). The fitting of the binding isotherm data (plotted as specific binding enthalpy *versus* receptor/ligand molar ratios) suggests a modest affinity (K_D = 3.5 μM; Table 2) and a 1:1 stoichiometry binding of c-di-GMP with *Xc*CLP (right, Fig. 4d). This binding affinity is within the range of physiological c-di-GMP levels in proteobacterial species[34] and is similar to the binding affinity in other known c-di-GMP receptors.[35] For example, affinities of 0.1 μM and 5.2–8.4 μM have been reported for the PilZ domain c-di-GMP sensors PlzD[36] and Alg44,[37] and affinities of 1.0 μM and 15–25 μM for the PelD[38] and FleQ transcription factor,[34] respectively. However, it should be noted that the ITC experiment of *Xc*CLP binding with c-di-GMP had to be carried out under high salt buffer, which may increase the K_D value due to the higher dielectric constant compared to that of low salt buffer.

Molecular modeling of *Xc*CLP–c-di-GMP complex

After proving that c-di-GMP is able to directly bind with *Xc*CLP and that this results in its dissociation from DNA, we further carried out an extensive docking study to identify potential c-di-GMP binding sites in *Xc*CLP. Interestingly, most of the docked c-di-GMP turn out to be residing in a local positively charged space between the bottom of helix αC and the top of helix αD (Fig. 5a), a region that has been demonstrated to exert the most prominent effect on the DNA-binding strength of *Ec*CRP.[31] In the docked model, c-di-GMP binds in a cis configuration, with both guanine bases oriented parallel with each other (Fig. 5b).[36] The top guanine base forms three specific H-bonds (between the side-chain carboxylate of D70′ and the N1 and N2 atoms of guanine base, and between the side-chain guanido HN of R166 and the O6 of guanine base), while the bottom guanine base forms one specific H-bond (between backbone HN of R154 and O6 of guanine base) with *Xc*CLP, respectively. Another key c-di-GMP recognition motif involves residues R150 and R154 from helix αC. The side chain of R154 is found to be extended and interdigitated between the two guanine bases, with one of its guanido HNs forming a H-bond with the c-di-GMP phosphate oxygen atom.[36] The side chain of R150 is also found to be extended and forms a salt bridge with the second c-di-GMP phosphate oxygen atom (Fig. 5b). The positively charged guanidine group of R154 is able to make a π−π interaction with the six-member ring of the lower guanine base, which is stacked below by the extended side chain of K151 (Fig. 5b). Similarly, the side chain of H169 is also found to be situated in hydrophobic interaction distance to the five-member ring of the upper guanine base. The c-di-GMP is thus stably wedged in the docked space, forming seven specific H-bonds and a variety of hydrophobic interactions with *Xc*CLP. More importantly, c-di-GMP binding also seems to stabilize the core conformation of *Xc*CLP by forming four extra specific salt bridges between the side-chain atoms of D70′ and R166 and the side-chain atoms of R154 and D170 (Fig. 5b) from this modeling result.

Table 2. Binding affinities of native and mutant CLPs with c-di-GMP determined by ITC under high salt buffer

	K_D (M)	Fold	$\triangle H$ (cal/mol)	$\triangle S$ (cal/mol per degree)
Native CLP	3.5E-6	1	−1.4E3	20.7
K173A/E174A/E176A	3.8E-6	1	−1.35E3	18.5
D70A	9.5E-5	27	−1.5E4	−15.8
R154A	3.0E-5	8	−2.5E4	−63.5
R166A	4.0E-5	11	−1.86E4	−40
D170A	3.8E-5	11	−1.92E4	−44
R166A/D170A	8.8E-5	25	−2.48E4	−64

High-salt buffer: 250 mM NaCl, 20 mM Tris (pH 8.0), and 100 mM LiCl.

Binding analyses using variant proteins with alanine substitutions for key residues support the model for c-di-GMP binding to *Xc*CLP

The importance of *Xc*CLP residues that putatively interact with c-di-GMP as revealed from modeling studies was examined experimentally. The binding of c-di-GMP with *Xc*CLP variants D70A, R154A, R166A, D170A, and R166A/D170A was measured by ITC. The results (Table 2) indicated the affinity of all these variant proteins was reduced by between 8- and 27-fold, although more drastic reduction in affinity for the R166A/D170A double mutant is expected. In contrast, c-di-GMP binding to the *Xc*CLP triple variant (K173A/E174A/E176A), which has alterations in residues not involved in c-di-GMP binding as revealed from the modeled complex, was unaltered.

The importance of binding of c-di-GMP by these residues to the inhibition of *Xc*CLP binding to promoter DNA was also addressed by competition SPR experiments. For these experiments, native *Xc*CLP and variants (0.4 μM) alone or in the presence of increasing concentrations of c-di-GMP (0, 0.1, 0.2, 0.4, 0.8, and 2 μM) were applied to a

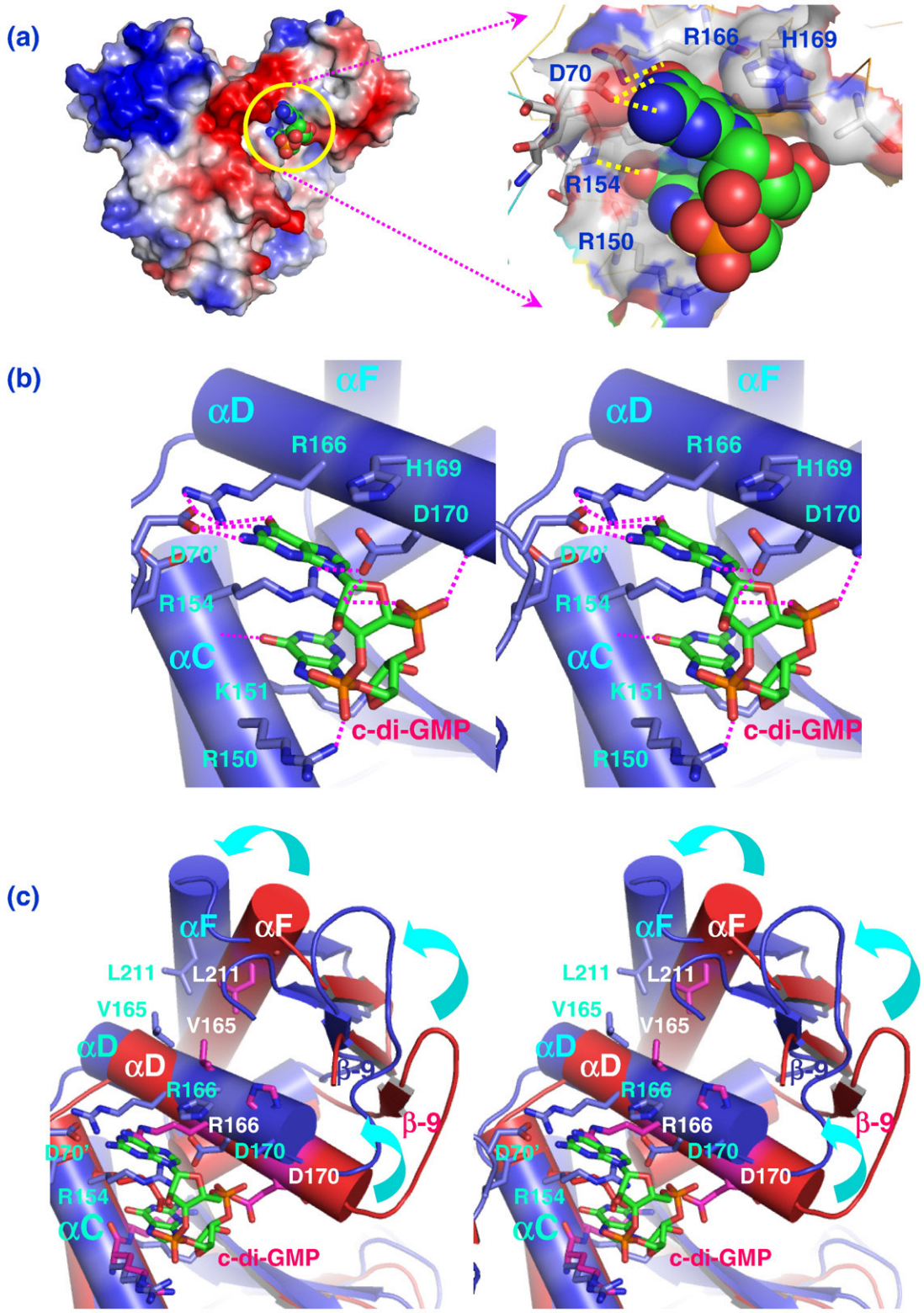

Fig. 5. Docked model of c-di-GMP–*Xc*CLP complex. (a) *Xc*CLP dimer drawn in electrostatic surface (positive, blue, and negative, red), with the c-di-GMP molecule drawn in van der Waals (nitrogen atoms in blue, oxygen atoms in red, and carbon atoms in green). The docked region is circled in yellow and expanded in a close-up at right. Specific H-bonds between c-di-GMP and *Xc*CLP are indicated by yellow dotted lines. (b) Specific interactions between c-di-GMP and *Xc*CLP drawn in cartoon representation. Residues participating in these interactions are drawn as sticks, with H-bonds or salt bridges shown as dotted red lines. (c) Superimposition between the DNA-binding domains of apo *Xc*CLP (cartoons in red) and the *Xc*CLP–c-di-GMP complex (cartoons in blue). Carbon atoms of the apo *Xc*CLP are colored pink, while those in the c-di-GMP–*Xc*CLP are colored gray. Binding of c-di-GMP seems to change the conformation of *Xc*CLP to an inactive open form (blue) compared to the active closed form (red) of apo *Xc*CLP (indicated by curved cyan arrows).

promoter DNA chip. As shown in Supplementary Fig. S4, an IC_{50} value of approximately 0.2 μM was obtained for both the native *Xc*CLP and the K173A/E174A/E176A triple variant, indicating that the residues not participating in c-di-GMP binding do not influence the competition. However, although *Xc*CLP D70A, R154A, R166A, D170A, and R166A/D170A variants all bind promoter DNA with affinities that are very similar to that of the native protein, this binding was not sensitive to the presence of c-di-GMP even at 2 μM (Supplementary Fig. S4). These competition SPR results thus gave further support for the importance of D70, R154, R166, and D170 residues in binding c-di-GMP.

Binding of c-di-GMP may affect helix αD of *Xc*CLP to inactivate DNA binding

Contrary to the case of *Ec*CRP, in which the binding of cAMP was found to induce the structural rearrangements to a closed form required for DNA-binding,[30] binding of c-di-GMP appears to trigger the intrinsically active *Xc*CLP conformation into an open form or inactive state, hence abolishing its DNA-binding ability. This effect is best shown in the superimposition figure of the HTH motifs between the apo *Xc*CLP (colored orange) and the modeled *Xc*CLP–c-di-GMP complex (colored blue, Fig. 5c). It is likely that c-di-GMP binds in the space between helices αC and αD, pushing upward several crucial residues such as R166 and D170 located in the helix αD. The most important one to be affected is probably residue V165, which is also located in helix αD and found to interact strongly with residue L211 located in the DNA-contacting helix αF.[31] The upper movements of residue V165 will thus push upward the DNA-contacting helix αF, resulting in an open and inactive conformation for *Xc*CLP (annotated by curved cyan arrows in Fig. 5c, see also the region circled in green in Fig. 2a), and explaining the inactivation of DNA binding of *Xc*CLP triggered by c-di-GMP binding.

Discussion

Transcriptional regulators belonging to the CRP/FNR superfamily are generally activated by a small effector such as cAMP, O_2, or others.[26] Here we have described the structural basis for the binding of promoter DNA by *Xc*CLP, which unusually occurs in the absence of any ligand. Furthermore we have addressed the molecular basis of the influence of c-di-GMP in inhibition of DNA binding by *Xc*CLP. The findings provide a mechanistic link between cell–cell signaling involving the Rpf–DSF system, which acts to modulate cellular levels of c-di-GMP,[32] and regulation of expression of particular virulence genes. More importantly, the appreciation that a member of the CRP family of proteins responds to c-di-GMP as a ligand expands the range of c-di-GMP plain effector proteins identified in bacterial cells beyond those already known, which include the PelD regulator from *P. aeruginosa*,[38] FleQ regulator from *P. aeruginosa*,[34] and various proteins with a PilZ domain.[35–37]

The requirements to switch a cAMP-dependent CRP to a cAMP-independent CRP* variant have been well fulfilled in the native *Xc*CLP sequence that forms a stable tertiary structure intrinsically adapted for cognate promoter DNA binding. Variations that lead to the cAMP-independent transcription by *Ec*CRP*, such as changes of residues 139 (located within the hinge region) and 142 (located in the αD helix adjacent to the hinge) to polar residues,[31] are observed in our native *Xc*CRP crystal structure as shown in Fig. 3c. In addition, the requirement for a bulky residue at position 145 of the αD helix of *Ec*CRP* is also satisfied by V165 in *Xc*CLP.[31] Furthermore, the proposed unique domain–domain interactions between residue Y64 in the β5 strand and residue E172 in the αD helix that can contribute to the *Ec*CRP* stability[30] is also well reflected in our crystal structure (Fig. 3b). However, in *Xc*CRP, it is R195 (corresponding to residue Q175 in *Ec*CRP) that causes rotation of the side chain of residue E192 (which corresponds to residue E172 in *Ec*CRP). The two side-chain oxygen atoms of E192 then connect the DNA binding domain with the N-terminal domain by forming two H-bonds with R195 located at the αD helix and with Y79 located at the β5 strand, respectively. Recently, a G145S variant of PrfA, the key virulence regulator from the Gram-positive bacterium *Listeria monocytogenes*, has been found to exhibit better DNA-binding affinity through the stabilization of the HTH motif.[39] The G145S mutant of this constitutively active PrfA protein is akin to the A145T mutant of *Ec*CRP. Both mutations are located in helix αD, with a similar activation mechanism. This is also the case for *Xc*CLP, with the similar position being altered to another bulky V165 residue as described above.

Cyclic-di-GMP seems to be less effective in binding *Xc*CLP ($K_D = 3.5 \times 10^{-6}$, Table 2) than binding promoter DNA ($K_D = 1.4 \times 10^{-8}$, Table 1), and one may wonder whether c-di-GMP is effective enough to compete with promoter DNA for *Xc*CLP binding. However, it is important to note that these two binding affinities were measured by different biophysical methods under different salt concentrations. Cyclic-di-GMP–*Xc*CLP binding was measured using ITC_{200} that requires a higher stock *Xc*CLP concentration (25 μM) and hence a higher salt concentration to dissolve it. Instead, c-di-GMP–DNA binding was measured using SPR that requires only a lower *Xc*CLP concentration (2 μM) and hence a lower salt concentration. When the *Xc*CLP binding and the K173A/E174A/E176A triple mutant binding with promoter DNA were carried out under similar high salt buffer, it was found that their K_D values do increase by approximately 26-fold (Table 1), reflecting the increasing dielectric constants of the higher salt buffer to shield the binding strength between two charged molecules. In fact, when the competition SPR experiments were carried out at the same low salt concentration, we found that c-di-GMP is indeed able to compete efficiently with

promoter DNA for binding *Xc*CLP with an IC_{50} of approximately 0.2 μM (Supplementary Fig. S4).

Together, the docking analysis and the experimental findings indicate that D70, R154, R166, and D170 of *Xc*CLP are required for c-di-GMP binding. Examination of the amino acid sequence of *Xc*CLP indicates that R154 and D170 are present within motifs with some similarity to those required for c-di-GMP binding by PilZ domains; specifically ^{150}RxxxR^{154} motif and the DxS sequence in the ^{170}D/NxSxxG motif of PilZ. This limited similarity and the additional involvement of the residues D70 and R166 may suggest that the *Xc*CLP binding site for c-di-GMP is novel, although direct evidence such as the determination of the crystal structure of the *Xc*CLP–c-di-GMP complex is necessary to establish this notion.

It is intriguing to note that nature has evolved very similar regulatory proteins (*Ec*CRP and *Xc*CLP) that are controlled in a divergent fashion by different cyclic mono- or dinucleotides. Our findings suggest that this is not simply due to alteration in the cyclic mononucleotide-binding pocket, because c-di-GMP binds to *Xc*CLP at a different site from cAMP binding to *Ec*CRP. A possible evolutionary pathway between *Ec*CRP and *Xc*CLP (Fig. 6) envisages evolution of *Ec*CRP, which is only active in transcriptional regulation in the presence of cAMP, to an *Ec*CRP*-like protein through accumulation of mutations leading to structural alterations that mimic the cAMP-induced conformational changes of *Ec*CRP. Further mutations render the intrinsic action of the *Ec*CRP*-like protein *Xc*CLP in binding to promoter DNA responsive to c-di-GMP. Since no adenylate

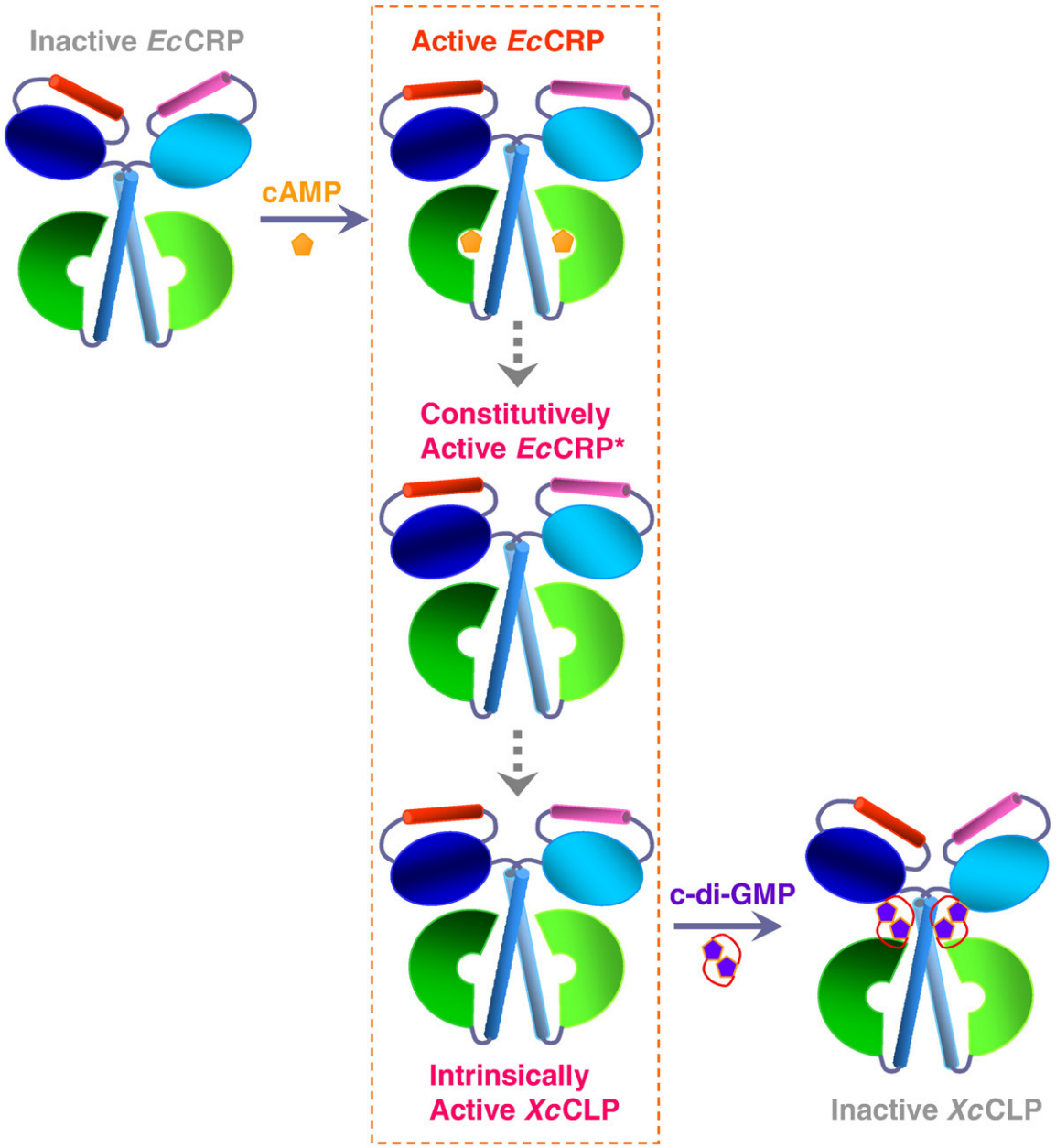

Fig. 6. Cartoon models of sequence evolution from *Ec*CRP to *Xc*CLP. The evolution pathway is boxed in dotted orange.

cyclase or CRP gene can be detected in the genomes of *Xanthomonas* spp., the c-di-GMP/CLP pair rather than the cAMP/CRP pair may be the major player in regulating gene expression in *Xanthomonas* spp.

In conclusion, we propose that the influence of the second messenger c-di-GMP on the promoter binding capability of the transcription factor *Xc*CLP is the mechanistic link between cell–cell signaling mediated by the Rpf/DSF system and the expression of specific pathogenicity genes in *Xcc*. This mechanism of regulation by c-di-GMP may extend to other xanthomonads including the clinically relevant *Stenotrophomonas maltophilia*,[40,41] which all have CLP proteins that are highly related to *Xc*CLP. It remains to be seen whether more distantly related members of this family from unrelated bacteria have similar structure and are similarly regulated. Quenching bacterial quorum-sensing pathways is becoming a new paradigm for developing the next-generation drugs to combat pathogenic bacteria without potentially eliciting drug resistance.[42] The DSF/Rpf signaling network in *S. maltophilia* may serve as a good target for such drug development.[43] Many potential targets for interference are possible, including those involved in quorum-sensing signal generation, signal detection, or signal transduction.[44,45] *Sm*CLP may represent an attractive downstream target for attenuating the *S. maltophilia* pathogenicity if a suitable inhibitor can be found.

After completion of this article, a paper describing a similar inhibition of c-di-GMP against DNA binding by CLP from *Xanthomonas axonopodis* pv. *citri* was published.[46] A somewhat weaker binding affinity of *Xa*CLP toward its target DNA than *Xc*CLP (60 nM *versus* 14 nM) and a somewhat stronger *Xa*CLP binding toward c-di-GMP than *Xc*CLP (1 μM *versus* 3.5 μM) were reported. These small differences could be due in part to differences in salt and buffer condition utilized. A commentary regarding the significance of this finding has also followed. Interestingly this identifies the questions of structure–function and c-di-GMP binding that the submitted paper addresses as being of great importance.[47]

Experimental Procedures

Cloning, expression, and purification of native and variant *Xc*CLPs

Two primers, one forward (5′-GCCTACATATGAGCCTAGGGAACACGAC-3′), and one reverse (5′-GCTCTAGATTAGCGCGTGCCGTACAACAC-3′) containing sequences for the NdeI and XhoI restriction sites, were designed on the basis of the genome sequence of *Xanthomonas campestris* pv. *campestris* (*Xcc*) strain 17. DNA fragment encoding the *clp* gene was PCR-amplified and cloned into the NdeI–XhoI sites of the pET32a vector. *E. coli* BL21(DE3) cells harboring the recombinant plasmids were grown at 310 K in 800 ml of LB medium containing ampicillin (100 μg/ml) to an OD_{600} of 0.7–0.9. Expression of the target *clp* gene was induced by the addition of 0.5 mM isopropyl-β-D-thiogalactopyranoside (IPTG) at 301 K for 8 h. Overexpressed *Xc*CLP protein with a His_6-tag at the C-terminal end was purified by an immobilized nickel-ion column (Qiagen, Valencia, CA) and analyzed by SDS-PAGE. The purified *Xc*CLP exhibits a molecular mass of about 26 kDa, corresponding to the calculated mass of tagged translation products. The D70A, R154A, R166A, D170A, and R166A/D170A variants for confirming residues essential for intrinsic *Xc*CLP–promoter binding, the E99A, R150A, E99A/R150A, K195A, D162A, and V165A mutants for confirming residues participating in c-di-GMP binding, and the K173A/E174A/E176A triple variant as a control were prepared by using the QuikChange site-directed mutagenesis kit (Stratagene) and the appropriate primers,[48] with the resulting sequences confirmed by DNA sequencing. Due to the lower solubility of *Xc*CLP, a higher salt concentration of 250 mM NaCl and 100 mM LiCl in 20 mM Tris (pH 8.0) buffer was applied during its purification procedure.

Crystallization of *Xc*CLP

Purified *Xc*CLP was concentrated using the Amicon 3 kD at 20 °C to a final stock concentration of 10 mg/ml in 250 mM NaCl, 100 mM LiCl, 20 mM Tris (pH 8.0) buffer and 1% glycerol. The stocked protein solution was screened for crystal formation in 600 different conditions using a robot system. Initial crystallization condition of 25% PEG (polyethylene glycol) 3350, 0.2 M Li_2SO_4, and 0.1 M Tris buffer (pH 8.5) was identified. The screened condition was further adjusted manually to improve the crystal quality, leading to a final condition of 23% PEG 3350, 0.15 M Li_2SO_4, and 0.1 M Tris buffer (pH 8.0). Several crystals of mutant *Xc*CLP large enough for X-ray diffraction were obtained after incubation for 1 week and diffracted to a resolution better than 2.3 Å.

Data collection and structural refinement

*Xc*UMPK crystals were flash-cooled at 100 K under a stream of cold nitrogen. X-ray diffraction data were collected using the National Synchrotron Radiation Research Center (NSRRC) beamline 13B1 in Taiwan. The data were indexed and integrated using HKL2000 processing software,[49] giving data that were larger than 97% complete with overall R_{merge} of 3.9% on intensities. A molecular replacement methodology by employing the AMoRe software[27] was carried out using the *Ec*CRP structure in the *Ec*CRP–DNA–cAMP complex (PDB code 1CGP) as the template. The model was manually adjusted using the XtalView/Xfit package.[50] CNS was then used for data refinement to a final R_{cryst} of 22.6% and R_{free} of 25.8%, respectively.[51] The crystals belong to the P_{21} space group. Based on the molecular mass of *Xc*CLP (25.6 kDa) and space group, it was assumed that the crystal contained four molecules per asymmetric unit. The assumption gives a V_M value of 2.42 $Å^3$/Da and a solvent content of 49.25%.[52] The detailed statistics about data collection and refinement of *Xc*CLP crystals are summarized in Table 3.

Activity assay

EMSA

The DNA-binding assay of native and *Xc*CLP were carried out by employing an EMSA method according to the previously reported protocol.[22] DNA probes used for EMSA analysis were prepared by PCR amplification of

Table 3. Statistics of data collection and structural refinement of native *Xc*CLP

Data collection	
Space group	P_{21}
Unit cell parameters	a = 67.687 Å, b = 67.694 Å, c = 110.372 Å, β = 104.20°
Wavelength (Å)	0.97622
Resolution range(Å)	30–2.28 (2.36 –2.28)
Total observations	183,340
Redundancy	4.3 (3.7)
Completeness (%)	97.1 (97.5)
R_{merge} (%)	3.9 (40.4)
$I/\sigma(I)$	24.5 (3.1)
Refinement statistics	
R_{free} test set size (%)	5
R/R_{free} (%)	22.6/25.8
Average *B*-factors (Å^2)	
All	48.13
Main chain	39.82
Side chain	52.13
Water molecules	48.65
Model content	
Residues	208×4
Water molecules	307
r.m.s.d. from ideal geometry	
Bonds (Å)	0.0066
Angles (°)	1.2267
Solvent content/Matthews coefficient (Å^3/Da)	49.25/2.42

Values in parenthesis are for the outermost shell, while the preceding values refer to all data.

the upstream region of the *Xcc engA* promoter, using labeled 5′-biotin-GCGATGTGATCGGTGCGGCAAT-3′ and 5′-biotin-GCTCGACACCCGA GCGCGGTAA-3′ oligonucleotides as primers. The amplified DNA fragment (102 bp) was purified from an agarose gel and applied for shift assay by using a LightShift™ Chemiluminescent EMSA kit (PIERCE). In competition EMSA experiments, different DNA probes containing both site I and site II *engA* promoter sequences (probe a), a single site II promoter sequence (probe b), and no promoter sequence (probe c), were used. Different amounts of c-di-GMP were incubated in the XcCLP–DNA complex mixtures.

SPR and competition SPR

For SPR experiments, a double-stranded biotinylated oligonucleotide containing the *Xc*CLP binding site I (−55 to −85 from the transcription initiation site) was immobilized onto a streptavidin-coated chip. Purified *Xc*CLP dissolved in a low salt buffer [80 mM NaCl, 20 mM Tris (pH 8.0), and 20 mM LiCl] of different concentrations ranging from 0.25 to 6 μM was passed through a DNA chip containing a double-stranded biotinylated oligonucleotide with the *Xc*CLP binding site I for 60 s, allowing the resonance signal to reach a plateau value. The protein-free low salt buffer was then passed over the chip to dissociate *Xc*CLP from the DNA chip, followed by washing of high salt solvent (1 M NaCl and 50 mM NaOH) to regenerate the chip. The dissociation constants (K_D) of the *Xc*CLP–DNA complex were determined using a 1:1 protein/ligand stoichiometry mode by the BIAevaluation software supplied by the vendor. For competition SPR experiments, *Xc*CLP (0.4 μM) alone or in the presence of increasing concentrations of c-di-GMP (0, 0.1, 0.2, 0.4, 0.8, and 2 μM) in the low salt buffer was injected over a flow cell of a BIAcore sensor chip containing the promoter double-stranded DNA. The steady-state binding responses recorded at the end of each injection for the native *Xc*CLP and the triple mutant were plotted against the concentration of c-di-GMP. IC_{50} values were obtained as the concentration of the c-di-GMP causing 50% decrease of the SPR signal compared to the corresponding negative control with zero competitor concentration.[53,54]

ITC

ITC experiments were carried out using an iTC_{200} microcalorimeter (MicroCal). A solution of 25.0 μM native *Xc*CLP or XcCLP mutants dissolving in high salt buffer was titrated with 13 injections at 3-min intervals of 3 μl each of a 0.375 mM stock solution of c-di-GMP in high salt buffer. Heat of binding (ΔH), the stoichiometry of binding (n), and the dissociation constant (K_D) were calculated from plots of the heat evolved per mole of ligand injected *versus* the molar ratio of ligand to receptor[55] using the software provided by the vendor. The ΔH and ΔS values obtained are listed in Table 2.

Molecular modeling and docking

To model the *Xc*CLP–c-di-GMP complex, we have carried out a docking analysis using the homemade GEMDOCK program[56,57] to predict the potential c-di-GMP binding sites in *Xc*CLP. The coordinates of c-di-GMP were obtained from the published structure (PDB code 2rde),[58] which was first minimized by SYBYL before docking. GEMDOCK was chosen for docking study because it is a well-developed tool that has been successfully applied in virtual screening[57,59] and in binding site prediction[60] and found to perform better than other comparative approaches, such as GOLD and FlexX, on a diverse data set of protein–ligand complexes.[61] Top-ranking models were then optimized using the SYBYL energy-minimization protocol. The DNA-bound *Xc*CLP model (see supplementary material) was used as the template for docking by c-di-GMP. Final results showed that most of the c-di-GMPs are situated at the hinge region of *Xc*CLP, and binding of c-di-GMP causes *Xc*CLP to be released from DNA-binding.

PDB accession number

The coordinates and structural factors of *Xc*CLP have been deposited in the PDB with accession number 3IWZ.

Acknowledgements

This work is supported by the Academic Excellence Pursuit grant from the Ministry of Education, and by the National Science Council, Taiwan, ROC (grants 97-2113-M005-005-MY3) to SH Chou. We appreciate the service of Structural Genomics Databases provided by the GMBD Bioinformatics Core (http://www.tbi.org.tw), NRPGM, Taiwan, ROC. We also like to thank the Core Facilities for Protein X-ray Crystallography in the Academia Sinica, Taiwan, for help in crystal screening, the NSRRC in Taiwan, and the SPring-8 Synchrotron facility in Japan for assistance in X-ray data collection. The NSRRC is a user facility supported by the

National Science Council, Taiwan, ROC, and the Protein Crystallography Facility is supported by the National Research Program for Genomic Medicine, Taiwan, ROC. Y. McCarthy, R. P. Ryan and J. M. Dow are supported by the Science Foundation of Ireland through a Principal Investigator Award (07/IN.1/B955) to J. M. Dow.

Supplementary Data

Supplementary data associated with this article can be found, in the online version, at doi:10.1016/j.jmb.2009.11.076

References

1. Jenal, U. (2004). Cyclic di-guanosine-monophosphate comes of age: a novel secondary messenger involved in modulating cell surface structures in bacteria? *Curr. Opin. Microbiol.* **7**, 185–191.
2. Jenal, U. & Malone, J. (2006). Mechanisms of cyclic-di-GMP signaling in bacteria. *Annu. Rev. Genet.* **40**, 385–407.
3. Romling, U. & Amikam, D. (2006). Cyclic di-GMP as a second messenger. *Curr. Opin. Microbiol.* **9**, 218–228.
4. Romling, U., Gomelsky, M. & Galperin, M. Y. (2005). C-di-GMP: the dawning of a novel bacterial signalling system. *Mol. Microbiol.* **57**, 629–639.
5. Barber, C. E., Tang, J. L., Feng, J.-X., Pan, M. Q., Wlison, T. J. G., Slater, H. *et al.* (1997). A novel regulatory system required for pathogenicity of *Xanthomonas campestris* is mediated by a small diffusible signal molecule. *Mol. Microbiol.* **24**, 555–566.
6. Ryan, R. P., Fouhy, Y., Lucey, J. F., Crossman, L. C., Spiro, S., He, Y.-W. *et al.* (2006). Cell-cell signaling in *Xanthomonas campestris* involves an HD-GYP domain protein that functions in cyclic di-GMP turnover. *Proc. Natl Acad. Sci. USA*, **103**, 6712–6717.
7. Slater, H., Alvarez-Morales, A., Barber, C. E., Daniels, M. J. & Dow, J. M. (2000). A two-component system involving an HD-GYP domain protein links cell–cell signalling to pathogenicity gene expression in *Xanthomonas campestris*. *Mol. Microbiol.* **38**, 986–1003.
8. Wang, L.-H., He, Y., Gao, Y., Wu, J. E., Dong, Y.-H., He, C. *et al.* (2004). A bacterial cell-cell communication signal with cross-kingdom structural analogues. *Mol. Microbiol.* **51**, 903–912.
9. He, Y.-W., Ng, A. Y.-J., Xu, M., Lin, K., Wang, L.-H., Dong, Y.-H. & Zhang, L.-H. (2007). *Xanthomonas campestris* cell–cell communication involves a putative nucleotide receptor protein Clp and a hierarchical signalling network. *Mol. Microbiol.* **64**, 281–292.
10. Ryan, R. P., Fouhy, Y., Lucey, J. F., Jiang, B.-L., He, Y.-Q., Feng, J.-X. *et al.* (2007). Cyclic di-GMP signalling in the virulence and environmental adaptation of *Xanthomonas campestris*. *Mol. Microbiol.* **63**, 429–442.
11. Andrade, M. O., Alegria, M. C., Guzzo, C. R., Docena, C., Rosa, M. C. P., Ramos, C. H. I. & Farah, C. S. (2006). The HD-GYP domain of RpfG mediates a direct linkage between the Rpf quorum-sensing pathway and a subset of diguanylate cyclase proteins in the phytopathogen *Xanthomonas axonopodis* pv *citri*. *Mol. Microbiol.* **62**, 537–551.
12. Galperin, M. Y., Nikolskaya, A. N. & Koonin, E. V. (2001). Novel domains of the prokaryotic two-component signal transduction systems. *FEMS Microbiol. Lett.* **203**, 11–21.
13. Dow, J. M., Fouhy, Y., Lucey, J. F. & Ryan, R. P. (2006). The HD-GYP domain, cyclic di-GMP signaling, and bacterial virulence to plants. *Mol. Plant-Microbe Interact.* **19**, 1378–1384.
14. He, Y.-W., Xu, M., Lin, K., Ng, Y.-J. A., Wen, C.-M., Wang, L.-H. *et al.* (2006). Genome scale analysis of diffusible signal factor regulon in *Xanthomonas campestris* pv. *campestris*: identification of novel cell–cell communication-dependent genes and functions. *Mol. Microbiol.* **59**, 610–622.
15. He, Y.-W. & Zhang, L.-H. (2008). Quorum sensing and virulence regulation in *Xanthomonas campestris*. *FEMS Microbiol. Rev.* **32**, 842–857.
16. de Crecy-Lagard, V., Glaser, P., Lejeune, P., Sismeiro, O., Barber, C. E., Daniels, M. J. & Danchin, A. (1990). A *Xanthomonas campestris* pv. *campestris* protein similar to catabolite activation factor is involved in regulation of phytopathogenicity. *J. Bacteriol.* **172**, 5877–5883.
17. Dong, Q. & Ebright, R. H. (1992). DNA binding specificity and sequence of *Xanthomonas campestris* catabolite gene activator protein-like protein. *J. Bacteriol.* **174**, 5457–5461.
18. Passner, J. M. & Steitz, T. A. (1997). The structure of a CAP–DNA complex having two cAMP molecules bound to each monomer. *Proc. Natl Acad. Sci. USA*, **94**, 2843–2847.
19. Passner, J. M., Schultz, S. C. & Steitz, T. A. (2000). Modeling the cAMP-induced allosteric transition using the crystal structure of CAP-cAMP at 2.1 Å resolution. *J. Mol. Biol.* **304**, 847–859.
20. Lee, M.-C., Weng, S.-F. & Tseng, Y.-H. (2003). Flagellin gene *FliC* of *Xanthomonas campestris* is upregulated by transcription factor Clp. *Biochem. Biophys. Res. Commun.* **307**, 647–652.
21. Hsiao, Y.-M. & Tseng, Y.-H. (2002). Transcription of *Xanthomonas campestris prt1* gene encoding protease 1 increases during stationary phase and requires global transcription factor Clp. *Biochem. Biophys. Res. Commun.* **295**, 43–49.
22. Hsiao, Y.-M., Liao, H.-Y., Lee, M.-C., Yang, T.-C. & Tseng, Y.-H. (2005). Clp upregulates transcription *engA* gene encoding a virulence factor in *Xanthomonas campestris* by direct binding to the upstream tandem Clp sites. *FEBS Lett.* **579**, 3525–3533.
23. Hsiao, Y.-M., Zheng, M.-H., Hu, R.-M., Yang, T.-C. & Tseng, Y.-H. (2008). Regulation of the *peh*A gene encoding the major polygalacturonase of *Xanthomnas campestris* by Clp and RpfF. *Microbiology*, **154**, 705–713.
24. He, Y. W., Wang, C., Zhou, L., Song, H., Dow, J. M. & Zhang, L.-H. (2006). Dual signaling functions of the hybrid sensor kinase RpfC of *Xanthomonas campestris* involve either phosphorelay or receiver domain-protein interaction. *J. Biol. Chem.* **281**, 33414–33421.
25. Li, B., Wing, H., Lee, D., Wu, H.-C. & Busby, S. (1998). Transcription activation by *Escherichia coli* FNR protein: similarities to, and differences from, the CRP paradigm. *Nucleic Acids Res.* **26**, 2075–2081.
26. Korner, H., Sofia, H. J. & Zumft, W. G. (2003). Phylogeny of the bacterial superfamily of Crp-Fnr transcription regulators: exploiting the metabolic spectrum by controlling alternative gene programs. *FEMS Microbiol. Rev.* **27**, 559–592.
27. Navaza, G. (1994). AMoRe: an automated package for molecular replacement. *Acta Crystallogr. A*, **50**, 157–163.
28. Vagin, A. & Teplyakov, A. (1997). MOLREP: an automated program for molecular replacement. *J. Appl. Crystallogr.* **30**, 1022–1025.

29. McKay, D. B., Weber, I. T. & Steitz, T. A. (1982). Structure of catabolite gene activator protein at 2.9 Å resoultion. *J. Biol. Chem.* **257**, 9518–9524.
30. Harman, J. G., McKenney, K. & Peterkofsky, A. (1986). Structure-function analysis of three cAMP-independent forms of the cAMP receptor protein. *J. Biol. Chem.* **261**, 16332–16338.
31. Kim, J., Adhya, S. & Garges, S. (1992). Allosteric changes in the cAMP receptor protein of *Escherichia coli*: hinge reorientation. *Proc. Natl Acad. Sci. USA*, **89**, 9700–9704.
32. Ryan, R. P., Lucey, J., O'Donovan, K., McCarthy, Y., Yang, L., Tolker-Nielsen, T. & Dow, J. M. (2009). HD-GYP domain proteins regulate biofilm formation and virulence in *Pseudomonas aeruginosa*. *Environ. Microbiol.* **11**, 1126–1136.
33. Nguyen, B., Tanious, F. A. & Wilson, W. D. (2007). Biosensor-surface plasmon resonance: quantitative analysis of small molecule–nucleic acid interactions. *Methods*, **42**, 150–161.
34. Hickman, J. W. & Harwood, C. S. (2008). Identification of FleQ from *Pseudomonas aeruginosa* as a c-di-GMP-responsive transcription factor. *Mol. Microbiol.* **69**, 376–389.
35. Hengge, R. (2009). Principles of c-di-GMP signalling in bacteria. *Nat. Rev. Microbiol.* **7**, 263–273.
36. Benach, J., Swaminathan, S. S., Ramayo, R., Handelman, S. K., Folta-Stogniew, E., Ramos, J. E. *et al.* (2007). The structural basis of cyclic diguanylate signal transduction by PilZ domains. *EMBO J.* **26**, 5153–5166.
37. Merighi, M., Lee, V. T., Hyodo, M., Hayakawa, Y. & Lory, S. (2007). The second messenger bis-(3′-5′)-cyclic-GMP and its PilZ domain-containing receptor Alg44 are required for alginate biosynthesis in *Pseudomonas aeruginosa*. *Mol. Microbiol.* **65**, 876–895.
38. Lee, V. T., Matewish, J. M., Kessler, J. L., Hyodo, M., Hayakawa, Y. & Lory, S. (2007). A cyclic-di-GMP receptor required for bacterial exopolysaccharide production. *Mol. Microbiol.* **65**, 1474–1484.
39. Eiting, M., Hageluken, G., Schubert, W.-D. & Heinz, D. W. (2005). The mutation G145S in PrfA, a key virulence regulator of *Listeria monocytogenes*, increases DNA-binding affinity by stabilizing the HTH motif. *Mol. Microbiol.* **56**, 433–446.
40. Johnson, A. P. & Duckworth, G. J. (2008). The emergence of *Stenotrophomonas maltophilia*. *Br. Med. J.* **336**, 1322.
41. Looney, W. J., Narita, M. & Muhlemann, K. (2009). *Stenotrophomonas maltophilia*: an emerging opportunist human pathogen. *Lancet Infect. Dis.* **9**, 312–323.
42. Clatworthy, A. E., Pierson, E. & Hung, D. T. (2007). Targeting virulence: a new paradigm for antimicrobial therapy. *Nat. Chem. Biol.* **3**, 541–548.
43. Fouhy, Y., Scanlon, K., Schouest, K., Spillane, C., Crossman, L., Avison, M. B. *et al.* (2007). Diffusible signal factor-dependent cell-cell signaling and virulence in the nosocomial pathogen *Stenotrophomonas maltophilia*. *J. Bacteriol.* **189**, 4964–4968.
44. Rasmussen, T. B. & Givskov, M. (2006). Quorum-sensing inhibitors as anti-pathogenic drugs. *Int. J. Med. Microbiol.* **296**, 149–161.
45. Rasmussen, T. B. & Givskov, M. (2006). Quorum sensing inhibitors: a bargain of effects. *Microbiology*, **152**, 895–904.
46. Leduc, J. L. & Roberts, G. P. (2009). Cyclic di-GMP allosterically inhibits the CRP-like protein (Clp) of *Xanthomonas axonopodis* pv. *citri*. *J. Bacteriol.* **191**, 7121–7122.
47. Gomelsky, M. (2009). C-di-GMP-binding CRP-like protein: a spectacular new role for a veteran signal transduction actor. *J. Bacteriol.* **191**, 6785–6787.
48. Vandeyar, M. A., Weiner, M. P., Hutton, C. J. & Batt, C. A. (1988). A simple and rapid method for the selection of oligodeoxynucleotide-directed mutants. *Gene*, **65**, 129–133.
49. Otwinowski, Z. & Minor, W. (1997). Processing of the X-ray diffraction data collected in oscillation mode. *Methods Enzymol.* **276**, 307–326.
50. McRee, D. E. (1999). XtalView/Xfit—a versatile program for manipulating atomic coordinates and electron density. *J. Struct. Biol.* **125**, 156–165.
51. Brunger, A. T., Adams, P. D., Clore, G. M., DeLano, W. L., Gros, P., Grosse-Kunstleve, R. W. *et al.* (1998). Crystallography & NMR system: a new software suite for macromolecular structure determination. *Acta Crystallogr., Sect. D: Biol. Crystallogr.* **54**, 905–921.
52. Matthews, B. W. (1968). Solvent content of protein crystals. *J. Mol. Biol.* **33**, 491–497.
53. Viht, K., Schweinsberg, S., Lust, M., Vaasa, A., Raidaru, G., Lavogina, D. *et al.* (2007). Surface-plasmon-resonance-based biosensor with immobilized bisubstrate analog inhibitor for the determination of affinities of ATP-and protein-competitive ligands of cAMP-dependent protein kinase. *Anal. Biochem.* **362**, 268–277.
54. Rusnati, M., Urbinati, C., Caputo, A., Possati, L., Lortat-Jacob, H., Giacca, M. *et al.* (2001). Pentosan polysulfate as an inhibitor of extracellular HIV-1 Tat. *J. Biol. Chem.* **276**, 22420–22425.
55. Leavitt, S. & Freire, E. (2001). Direct measurement of protein binding energetics by isothermal titration calorimetry. *Curr. Opin. Struct. Biol.* **11**, 560–566.
56. Yang, J.-M. & Chen, C.-C. (2004). GEMDOCK: a generic evolutionary method for molecular docking. *Proteins: Struct. Funct. Bioinf.* **55**, 288–304.
57. Yang, J.-M., Chen, Y.-F., Yu, Y.-Y., Yen, K.-R. & Yang, Y.-L. (2007). Combinatorial computation approaches identifying tetracycline derivates as flaviviruses inhibitors. *PLoS ONE*, **12**, e428.1–e428.12.
58. Benach, J., Swaminathan, S. S., Tamayo, R., Handelman, S. K., Folta-Stogniew, E., Ramos, J. E. *et al.* (2007). The structural basis of cyclic diguanylate signal transduction by PilZ domains. *EMBO J.* **26**, 5153–5166.
59. Hung, H.-C., Tseng, C.-P., Yang, J.-M., Ju, Y.-W., Tseng, S.-N., Chen, Y.-F. *et al.* (2009). Aurintricarboxylic acid inhibits influenza virus neuraminidase. *Antiviral Res.* **81**, 123–131.
60. Yang, M.-C., Guan, H.-H., Yang, J.-M., Ko, C.-N., Liu, M.-Y., Lin, Y.-H. *et al.* (2008). Rational design for crystallization of β-lactoglobulin and vitamin D_3 complex: revealing a secondary binding site. *Cryst. Growth Des.* **8**, 4268–4276.
61. Jones, G., Willett, P., Glen, R. C., Leach, A. R. & Taylor, R. (1997). Development and validation of a genetic algorithm for flexible docking. *J. Mol. Biol.* **267**, 727–748.